EXPERIMENTAL AND NUMERICAL ANALYSIS OF A HELICOPTER GEAR BOX SUPPORT

Gerardus Janszen, Davide Cassani
Dipartimento di Ingegneria Aerospaziale, Politecnico di Milano
Milano, Italy

Abstract

A numerical analysis of a particular helicopter gear box support is presented. Different finite element models of the complete support have been created. Starting from a simplified model up to a more complex one, the sensitivity to the change of the elements used and the refinement of the mesh has been investigated to better understand the capability of the different models to predict correctly the stresses in the structure when subjected to the same loads as those applied in the experimental tests. Validation of each single model has been made by comparison with experimental data from different fatigue tests. Besides the classical way to measure the deformations, a much more recent method, the thermoelastic stress analysis (TSA), has been used to measure stress entity and its distribution. The major advantages in the adoption of a TSA are: it is a non destructive and non intrusive method for stress analysis; during the tests a direct qualitative and quantitative distribution of the principal stresses is available; it can be used to make a direct comparison with a finite element analysis. The paper illustrates in detail the FEM models and the possibility to use the TSA as a valid tool for a direct comparison between the experimental and numerical results, instead of the more classic way to compare FEM analysis results with those taken from strain gages measurements.

List of symbols

c_v	specific heat
E	Young's modulus
λ	thermoelastic coefficient
σ_1 σ_2 σ_3	principal stresses
$\sigma_{prin\text{-}max}$	maximum principal stress
$\sigma_{prin\text{-}min}$	minimum principal stress
$\sigma_{Von\ Mises}$	Von Mises stress
σ_{sn}	yield stress
σ_r	ultimate stress
v	Poisson's ratio
ρ	density
R	ratio of minimum to maximum load
T	temperature
με	micro-deformations

Introduction

Nowadays finite element methods are widely used in almost all engineering fields. In case of structural analysis, these methods can well predict stress and deformation distributions even when the model of the structure is coarsely defined. But when the details of the structure need to be verified, then a best choice between modelling and computational time in relation to the goodness of the final results has to be carried out even in the early phases of the design. An important structural detail of a helicopter gear box support has been analysed with different numerical models. These models can provide useful information on the best choice of the final model to be used in the stress-deformation analysis.

The support

The structure of the transmission support is made of a four web aluminium alloy casting machined central body with a cruciform shape (Fig.1). The central web is 250 [mm] long and has an average thickness of 2.5 [mm] except around a 108 [mm] diameter lightening hole where the thickness is 5 [mm]. A 3 [mm] thick stiffening brace has been placed in the load application plane.

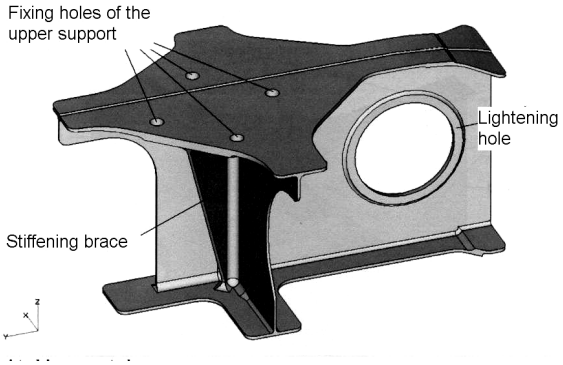

Fig. 1 – The central body of the gear box support

The lower side of the whole body is 3 [mm] thick while the upper side has a thickness variable from 3 to 8 [mm] where the loads from the gear box are introduced in the main structure. This is done by a titanium alloy element which provides the coupling between the support and the gear box strut (Fig. 2).
Thin aluminium alloy panels and angles are connected to the three shortest webs of the central body by means of rivets to give the structure its final stiffness. For the same reason another panel is located on the upper side. At the free ends of the stiffened webs and the main central web, shaped

plates provide for the fixing of the entire gear box support to the test table.

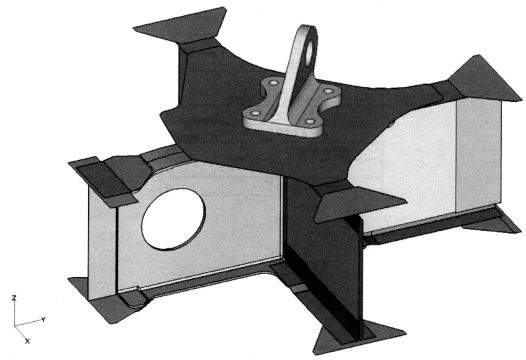

Fig. 2 – The complete gear box support

The central body is made of an Al 7475 aluminium alloy. The upper panel and the lateral constraining plates are made of an Al 7075 aluminium alloy. The remaining parts are made of an Al 2024 aluminium alloy. In the following table the material main mechanical characteristics, that have been used in the numerical models, are summarised.

Tab. 1 – Materials main mechanical characteristics

	σ_{sn} [MPa]	σ_r [MPa]	E [MPa]	ν	ρ [kg/dm^3]
Al 7475	421	496	70350	0.32	2.85
Al 7075	435	505	71086	0.29	2.85
Al 2024	310	448	71086	0.32	2.85
Ti	880	950	113800	0.34	4.43

Experimental tests

Different tests were carried out on the gear box support. One of these tests, that was reproduced with the numerical analysis, was an axial load fatigue test with constant amplitude and stress ratio R=0 at a frequency of 5 Hz. The maximum load was 81000 [N]. As described in the previous paragraph, the gear box support was constrained on a test table by four shaped plates connected to the support free ends. The load was applied by means of an hydraulic jack in the plane of the stiffening brace and tilted 50° upward.
A total of four single grid strain gages and five strain rosettes were used to measure the deformations during the tests. They were positioned close to the areas were the maximum stresses were expected (Fig.3). The strain rosettes R1 and R3 were located close to the hole and in a diametrically opposite position where a stress concentration was supposed to occur. The strain rosette R2 was located, between the hole and the branch of the webs, on the central web and R4 on the web perpendicular to this one. The strain rosette R5 was located on the stiffening panel of the shortest web. The four single grid strain gages were located on the opposite sides of the stiffening brace .

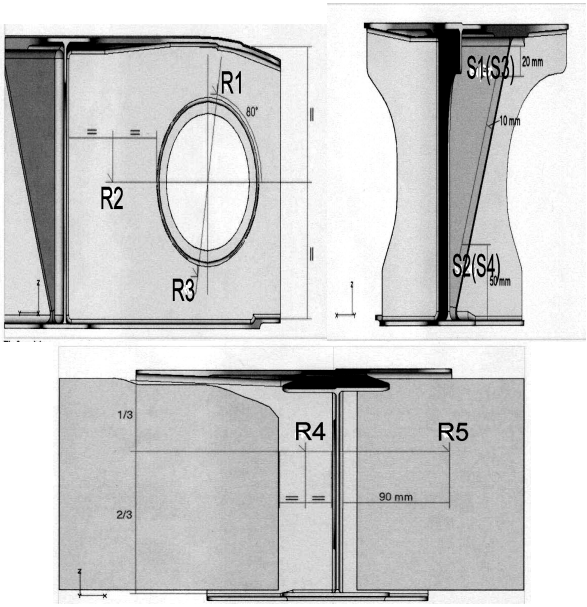

Fig. 3 – Strain gage positioning

In the following table the results of the experimental test are shown.

Tab. 2 – Results of the experimental test

Strain Gage	$\sigma_{prin-max}$ [MPa]	$\sigma_{prin-min}$ [MPa]	$\sigma_{Von\ Mises}$ [MPa]	με
S1	-	-	-	1425.18
S2	-	-	-	570.84
S3	-	-	-	1364.29
S4	-	-	-	535.39
R1	115.6	-33.5	135.4	-
R2	47.9	-47.7	82.8	-
R3	81.5	-28.5	98.9	-
R4	23	0	23	-
R5	68.4	-93	140.3	-

Thermoelastic tests

Thermoelastic stress analysis (TSA) is a quite recent but continuously evolving technique used to carry out stress analysis [Refs. 1,2,3,4,5]. TSA can be considered a complementary way to the more classical strain gage measurement method. It is able to give immediate visualization of the principal stresses distribution. Being a non destructive and non intrusive method, it was considered particular efficient for this type of tests. The TSA technique

uses an extremely sensitive infra-red array camera which is capable of measuring minute temperature changes induced in the component during dynamic loading. Exactly as what happens in a gas when it is subjected to a change in its pressure, in a solid a change in the stress causes a change in its temperature. This phenomenon is related to as the thermoelastic effect of the solids. If the load is applied statically the solid would have time to lose the heat so that the temperature would be constant; therefore to have a variation of the temperature that depends directly from the stress, the load must be applied dynamically at sufficiently high frequencies, to guarantee an adiabatic condition of the structure's material. In this conditions the temperature variation is proportional to the volume change, which is related to the first stress invariant of the stresses which is the sum of the three principal stresses:

$$\Delta T = -K_0 \bullet T_0 \bullet \Delta\sigma$$

where:

$$\Delta\sigma = \Delta(\sigma_1 + \sigma_2 + \sigma_3)$$

$$K_0 = \frac{\lambda}{\rho \bullet c_v}$$

Thermodynamic theory predicts in most of the cases that tensile loads produce a decrease of the temperature while the opposite occurs with compressive loads. The following values give an idea of the temperature variation needed to produce a 1 [MPa] change:

Aluminium alloy Al 7075 ΔT = 2.8 [mK]

Common Steel ΔT = 1[mK]

The dynamic loads applied in the thermoelastic tests ranged within ± 81000 [N]. The support was black painted to avoid reflection and heat loss problems.
The following figure shows the attemperation around both sides of the central web hole during the tensile and compressive loads.

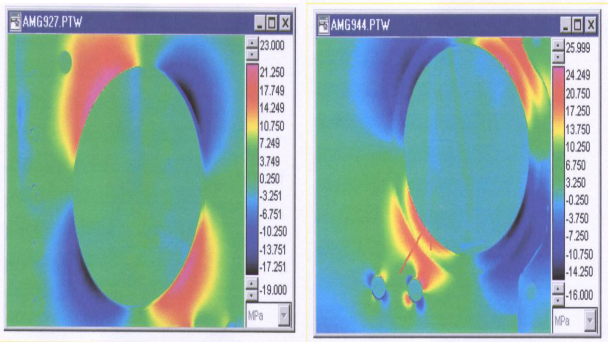

Fig. 4 TSA image of the first stress invariant around both sides of the hole with the tensile-compressive loads.

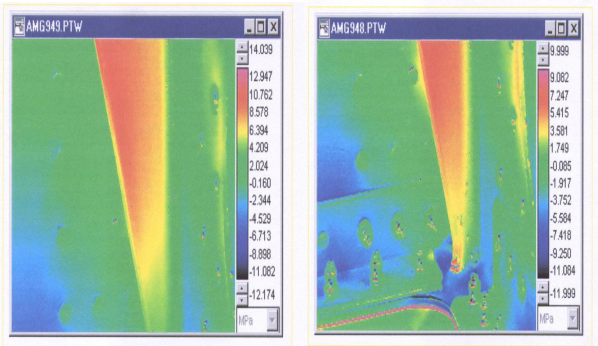

Fig. 5 TSA image of the first stress invariant on the stiffening brace.

A consideration must be made on the fact that the support is made of an aluminium alloy. This material has a great heat exchange coefficient which leads to a fast thermal equilibrium with the test room condition. This implies that the real values are greater than those indicated in the figure because a part of the thermal energy has been transmitted to the environment.

FEM models

For the finite element analysis the following commercial software was used: MSC FEMAP 8.3 as pre and post-processor, MSC PATRAN 2000 as post-processor and NASTRAN as solver [Refs. 6,7,8,9]. The gear box support was modelled in different ways by using the typical structural elements present in NASTRAN, starting from a very simplified model up to a more complex one.
In the first model only the rough geometry, considering the mean surfaces of the support subassemblies, has been reproduced using 5x5 [mm] bidimensional *plate* elements. The real value of the thickness has been assigned to all those elements that reproduce the main central web and the stiffening panels fastened to the other three webs of the central body, and to most of the lower base and the outer parts of the upper base. The parts of the support where two or three panels are overlapped, a 75% of the total thickness was assigned to the *plate* element to have the correct bending stiffness of those parts of the real structure.
In the following figure (Fig. 6) the simplified model is shown. The different colour gradation define different element properties.
The coupling between the support and the gear box strut, and the four bolts have been modelled by the *RBE2 rigid* element. The load is applied to the master node of this element. This load has been applied statically and equal to the maximum value reached during the tests. The support has been constrained by freezing the translation of the most external nodes.

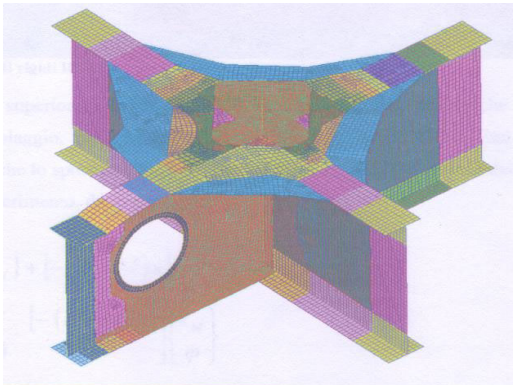

Fig. 6 Simplified FEM model of the support.

In the following table the maximum and minimum principal stresses and the error between the Von Mises stress and deformation of the numerical simulation and the experimental test are shown. The stresses indicated are obtained as the mean values of the stresses of the plate elements close to the position of the strain rosettes.

Tab. 3 – 1st model numerical results and comparison with the experimental test.

Strain Gage	$\sigma_{prin\text{-}max}$ [MPa]	$\sigma_{prin\text{-}min}$ [MPa]	$\sigma_{Von\ Mises}$	με
S1			-	63 %
S2			-	15.6 %
S3			-	63 %
S4			-	15.6 %
R1	101.1	-27.2	-13.4 %	-
R2	50.6	-25.3	-19 %	-
R3	72.4	-31.9	-6.4 %	-
R4	30.5	-10.8	61 %	-
R5	75.7	-65.8	-13.8 %	-

The area where the higher values of the stress are reached are those in correspondence with the brace and the upper part of the gear box support. Results show that this model is not able to follow the real behaviour in the most rigid parts of the support. Both the R4 strain rosette and the upper S1(S3) strain gage are overestimated. On the other hand, considering how the support is built up, it is important to understand how the load applied distributes on the central body in the four webs.
A further comparison between the stress distribution of the numerical analysis (Fig. 7) and the thermoelastic tests (Fig. 4), show the same stress distribution around the hole. The values of the first stress invariant are higher in the numerical simulation but attention must be put on the high heat exchange coefficient of the aluminium alloy which affects the real stress values. On the brace the results are different both in the stress distribution and in their values (Fig. 5 and Fig. 7).

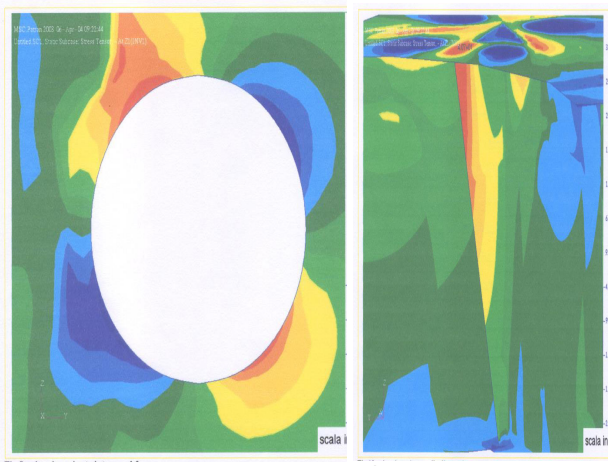

Fig. 7 First stress invariant from the numerical simulation around the hole and on the brace.

The second model has been created starting from the real geometry of the support. Every single part has been modelled using bidimensional *plate* elements of 3.5 [mm] side. The average surface has been taken out from the real geometry in correspondence of each single *plate* element and the thickness associated is exactly the thickness of that part of the support. The 2.5 [mm] diameter rivets have been modelled using the *bar* element. The application of the load and the constraint of the model has been simulated in exactly the same way as in the first model. In the following table the results of the numerical simulation and the errors with the results of the experimental test are shown. Also in this case the stresses indicated are obtained as the mean values of the stresses of the plate elements close to the position of the strain rosettes.

Tab. 4 – 2nd model numerical results and comparison with the experimental test.

Strain Gage	$\sigma_{prin\text{-}max}$ [MPa]	$\sigma_{prin\text{-}min}$ [MPa]	$\sigma_{Von\ Mises}$	με
S1			-	22.9 %
S2			-	17 %
S3			-	22.9 %
S4			-	17 %
R1	104.2	-32.4	-8.7 %	-
R2	51.6	-35.8	-8.1 %	-
R3	93.6	-43.3	22.5 %	-
R4	29.1	-6.2	42.3 %	-
R5	68.4	-77	-10.2 %	-

Comparing this results with those obtained with the previous model, it can be noticed that no particular benefits have been obtained. The same can be seen

comparing this results with those from the thermoelastic tests (Fig. 4 and Fig. 8)

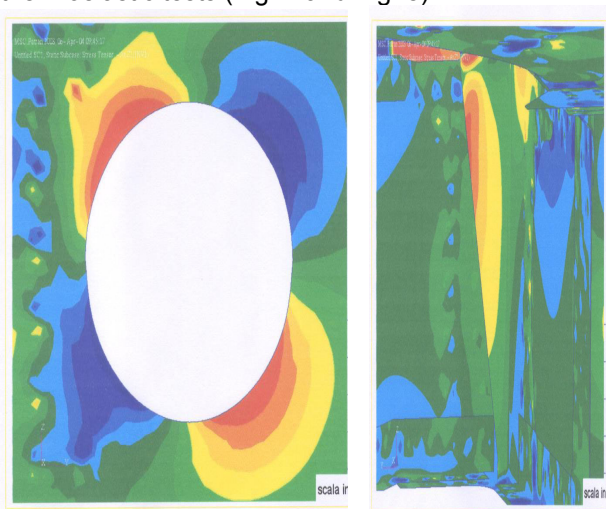

Fig. 8 First stress invariant from the numerical simulation around the hole and on the brace.

In the third model, the central body of the gear box support has been modelled with *solid tetrahedral* elements. This choice was due to their ease to tailor the complex geometry of the support. But, instead of dividing the volume of the support into a certain number of small tetrahedral volumes, which would have determined areas with a concentration of tetrahedral elements with a twisted or stretched form, especially in the junction areas, a more simple way has been followed. The external surface of the support has been divided in triangular elements and then extruded to fill up all the volume. This takes certainly much more time to create the mesh but the result is a more regular and homogeneous mesh in all the body. The dimension of the elements was constrained by the thickness of the vertical panels and at least two elements had to be put along the thickness so that the flexural behaviour could be well approximated. This has brought to an element that was of 1.25 [mm] side. To have a better approximation of the stress distribution it would have been better to use *tetrahedral* elements of the second order but this would have brought to an excessive huge model with too long computational times. The element which provides the coupling between the transmission support and the gear box strut has been modelled with *tetrahedral solid* elements too.

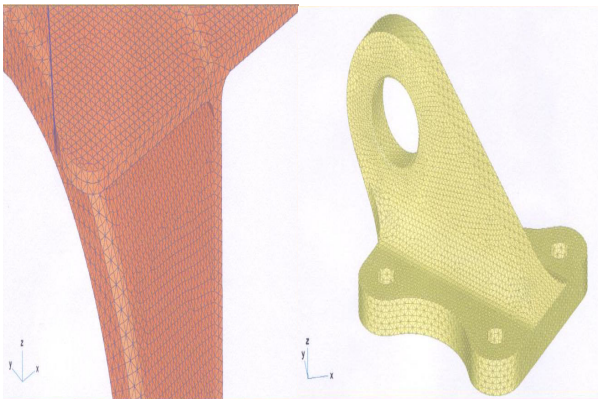

Fig. 9 Solid elements mesh of the central body and the upper coupling element

The load was applied to a fictitious node positioned in the centre of the eye of the upper coupling element and distributed to the nearby nodes with a *rigid* element. The same element has been used to reproduce the bolts. All the other parts have been modelled with *plate* elements using the mesh of the previous model. The connection between the panels has been done with *bar* elements.
In the following table the results of the numerical simulation compared with the experimental tests are shown.

Tab. 5 – 3rd model numerical results and comparison with the experimental test.

Strain Gage	$\sigma_{prin\text{-}max}$ [MPa]	$\sigma_{prin\text{-}min}$ [MPa]	$\sigma_{Von\ Mises}$	με
S1			-	15.3 %
S2			-	9.3 %
S3			-	15.3 %
S4			-	9.3 %
R1	116.3	-38.7	3.3 %	-
R2	62.4	-40.8	8.8 %	-
R3	88.2	-37.8	13.2 %	-
R4	27.8	-2.3	26.1 %	-
R5	67.7	-74.9	-11.9 %	-

The value of the stresses are overestimated by a mean value of 15% except on the vertical panel where the value is underestimated and this confirms that the use of *solid* elements in the central body has no influence on the vertical panel modelled with *plate* elements. Where the support is effectively much stiffer than other parts, the use of solid elements brings to an enhancement of the correlation with the experimental data. Also around the hole the correlation has been improved with respect to the results of the previous models. Even the distribution of the first stress invariant around the

hole and on the brace (Fig.10), if compared with those from the thermoelastic test (Fig.4), confirm this good correlation.

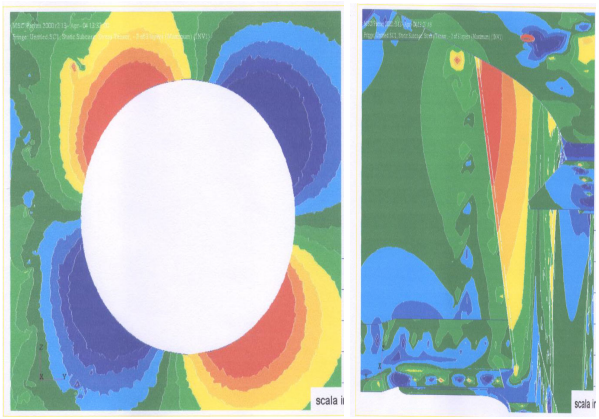

Fig. 10 First stress invariant from the numerical simulation around the hole and on the brace.

The last model, called the transition model, has been developed from the second model. Attention has been focused on the part of the central body where the strain rosette R1 around the hole was positioned. This was done because this area seemed to be the worst correlated with the experimental data by the simple models with respect to the solid elements model. The idea was to create a model not so heavy as this last model but that could better approximate the stress distribution around the hole. The area around the hole including a part of the upper sole has been modelled with second order tetrahedral elements (Fig. 11). The remaining part of the model is exactly the same as the second one. Particular attention has been given to the connection between this two differently modelled parts of the support to assure the continuity of the structure. This has been done using *rigid* elements that connected the nodes of the *plate* elements to the nodes of the *solid* elements.

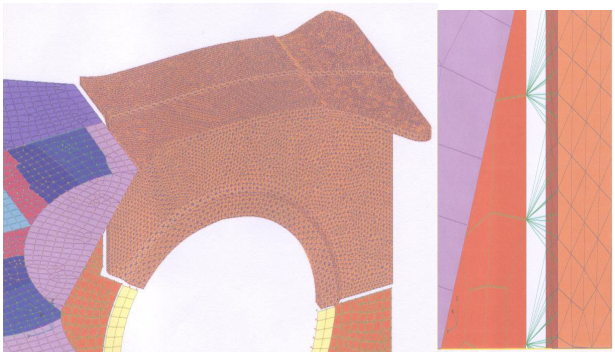

Fig. 11 Transition zone between the *plate* elements and the *solid* elements area

As with the previous models the results are shown in the following table.

Tab. 6 – 4th model numerical results and comparison with the experimental test.

Strain Gage	$\sigma_{prin\text{-}max}$ [MPa]	$\sigma_{prin\text{-}min}$ [MPa]	$\sigma_{Von\ Mises}$	με
S1			-	24.2 %
S2			-	19.95 %
S3			-	24.2 %
S4			-	19.95 %
R1	113	-43.7	3.5 %	-
R2	50.4	-36.7	-8.53 %	-
R3	92.1	-40.5	19 %	-
R4	30.1	-6.6	47.4 %	-
R5	66.7	-77.1	-11.1 %	-

From the results it can be noticed that the choice of the *solid* elements gives around the hole a better correlation with the experimental data. The other results are similar to those of the simple models.

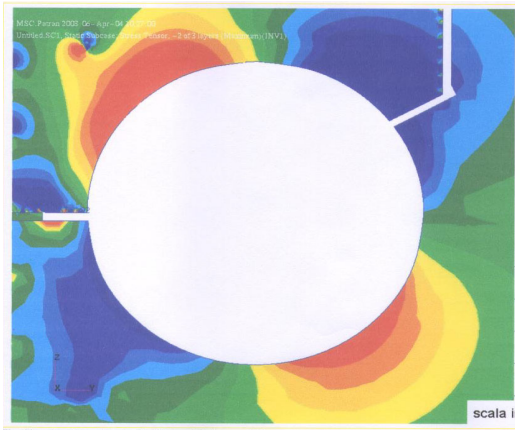

Fig. 12 First stress invariant distribution around the hole

Conclusions

Finite elements analysis of a gear box support have been carried out using different numerical models. From the comparison of the results of the numerical analysis with those of the experimental tests, it is clear how the lack of the measurement of the displacement of some peculiar points of the support, has brought to misunderstand the real stiffness of the whole support.

The main purpose of the presented work can be summarised in the following points of interest :

- stress distribution on the stiffening vertical panels
- stress distribution on the central body
- stress distribution around the hole

From the observation of the design of the support it is clear that the most severe loading condition is on the vertical panels attached to the webs and is due to the vertical component of the external load coming from the gear box strut. The larger stress, due to this load, as can be seen from the experimental tests, is on the smallest panel which is shorter and stiffer than the others. All the numerical models reproduce this fact but underestimate it. The simplified model gives the worst results, but the improvement up to the more complex model does not give any further improvement.
The simplified model and the implemented rivet model do not simulate correctly the structural behaviour of the brace and the central body, which represent the stiffest parts of the support, while the solid elements model show to well correlate with the experimental data even if still overestimates the value of the stress by approximately 8/15 %. And on the upper part of the brace, which is the most loaded, things go even better predicting the values properly.
On the main central web, the best correlation is achieved by using the *solid* elements model which gives errors which are not greater than 15 % with respect to the experimental data.
The pictures of the thermoelastic tests have been usefully adopted both as a direct mean of comparison between results from the numerical simulations and the experimental tests, and in the creation of the different finite element models. The global vision they give can be used quite directly to locate, in the modelling phase, the areas where the mesh has necessarily to be refined. Moreover this data has been used to identify the best strain gage positioning for the fatigue tests.
Finally it is useful to take a look at the following table in which the complexity of the different models, the modelling time and the computational time are shown.

Tab. 7 Comparison between the different models.

	Node n°	Element n°	Comp. time	Mod. time
Simple	16265	16074	1min 19sec	20h
Rivets	41443	39836	1 min 21 sec	48h
Solid	392223	1681980	1h27min35sec	120h
Trans	230295	156344	31min 08sec	10h

It must be pointed out that the modelling time for the *solid* elements model it must be pointed out that normally the mesh can be directly produced once you have a CAD drawing of the geometry. In this case this CAD file was not available and this has brought up the time to the value shown.

As a final comment, even if *solid* elements have been shown to be the best choice to simulate the support that has been analysed, good results can be achieved with a coarse definition of some parts of a structure, that act as load transmitters, and a refinement only in those parts that are of real interest in the stress analysis.

References

1) Stanley, P. and Chan, W. K., "Quantitative Stress Analysis by Means of the Thermoelastic Effect", *J. Strain Analysis*, vol. 20, pp. 129-137, 1985.
2) Cummings, W. M. and Harwood, N., "Design Analysis of Engineering Structures Using SPATE", *First Scottish Design Engng. Conf.*, 1985, Apr.
3) Cummings, W. M., "Thermoelastic Stress Analysis", *Engineering*, vol. Technical File 132, 1985, Feb.
4) Harwood, N. and Cummings, W. M., "Application of Thermoelastic Stress Analysis", *Strain*, vol. 22, pp. 7-12, 1986
5) Everett, G. M., "Comparison between the Thermoelastic Method and other Experimental Techniques for Stress Measurement", *Stress and Vibration: Recent* Developments in Industrial Measurement and Anal., vol. 1084, pp. 54-58, 1989, Mar.
6) MSC FEMAP 8.3 manual
7) MSC PATRAN 2000 manual
8) Quick Reference Guide of NASTRAN
9) H. G. Schaeffer, “MSC/NASTRAN – Static and Normal Mode Analysis”